Ultrasonics Sonochemistry 114 (2025) 107248

Contents lists available at ScienceDirect

Ultrasonics Sonochemistry

journal homepage: www.elsevier.com/locate/ultson

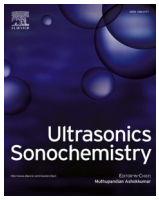

Ultrasound-assisted enzyme extraction of Dendrobium Officinale polysaccharides: Extraction process, characterization, immunomodulatory effects

Hengpu Zhou [1], Yingjie Dong [1], Zhangyun Wu [1], Xi Peng, Meiqiu Yan [*], Suhong Chen [*], Guiyuan Lv [*]

School of Pharmaceutical Sciences, Zhejiang Chinese Medical University, Hangzhou 310053, PR China

ARTICLE INFO

Keywords:
Ultrasound-assisted enzyme assay
Dendrobium Officinale polysaccharides
Characterization
Immunity
CD4/CD8
T-lymphocyte subpopulations

ABSTRACT

Dendrobium Officinale is a traditional Chinese medicinal and edible herb, and polysaccharides being its principal active components. We employed ultrasonic-assisted enzymatic extraction to obtain polysaccharides from Dendrobium Officinale (DOP) and optimized the extraction process using the GA-BP method. Subsequently, DOP was characterized using HPLC, SEM, and HPGPC. Finally, an immunocompromised mouse model induced by cyclophosphamide was adopted to evaluate the immunomodulatory effects. The results showed that the optimal extraction process of ultrasound-assisted enzyme method was 102 min ultrasonic extraction time, 48 °C extraction temperature, 1:80 material-liquid ratio, and 1600 U/g enzyme additions. The predicted polysaccharide yield was 29.64 %, and the actual polysaccharide yield was 29.71 ± 0.31 %. DOP is a white powder with pore-like structure, whose polysaccharide content is 90.66 ± 2.47 %, and with a composition of D-mannose, glucose, galactose, arabinose in a molar ratio of 74.17: 47.80: 9.03: 1. DOP has demonstrated the ability to improve the general condition of mice with cyclophosphamide-induced immunosuppression. It mitigates damage to the thymus and spleen tissues, increases white blood cell counts, regulates the ratio of T lymphocytes and the levels of related factors, enhances macrophage phagocytic function to improve nonspecific immune responses, and boosts the levels of immunoglobulins IgA and IgG to enhance specific immune function. Therefore, DOP can alleviate immunosuppression induced by cyclophosphamide.

1. Introduction

Dendrobium Officinale (DO) is a perennial herbaceous plant of Orchidaceae, widely distributed in tropical and subtropical regions of Asia, and the annual output of DO in China has exceeded 50,000 tons. DO belongs to both medicinal and food plants in China, it can be used for food and health care products, also can be used for raw food, tea, soup, wine, etc. Now there are about 170 kinds of DO health food were approved. Our traditional medicine believes that DO has the effect of benefiting the stomach and generating fluids, nourishing Yin and clearing heat[1]. Modern medical research shows that DO has antioxidant, anti-tumor, hypoglycemic, improve immunity and other effects [2–4].

There are many chemical components in DO, mainly can be divided into carbohydrates, flavonoids, bibenzyl, alkaloids and phenylpropanoids[5–7]. Among them, carbohydrates are an important ingredient in DO, the Chinese Pharmacopoeia 2020 version of DO content determination standard that is polysaccharide (not less than 25 %) and mannose content, it can be seen that the content of polysaccharides in DO is also closely related to its quality. With the in-depth study of polysaccharides in DO, its efficacy has been continuously explored, and its immune-regulating and anti-inflammatory effects are remarkable [8,9]. Our previous study found that Dendrobium Officinale polysaccharides (DOP) and its products can regulate immunity and inhibit

Abbreviations: DO, Dendrobium Officinale; DOP, Dendrobium Officinale polysaccharides; GA-BP, Genetic Algorithm-Back Propagation; IL-1, Interleukin-1; IL-6, Interleukin-6; IL-10, Interleukin-10; MSE, mean square error; HPLC, high performance liquid chromatography; IgA, Immunoglobulin A; IgG, Immunoglobulin G; H&E, Hematoxylin and eosin.

* Corresponding authors at: School of Pharmaceutical Sciences, Zhejiang Chinese Medical University, Hangzhou 310053, PR China (G. Lv).
E-mail addresses: meiqiuyan@163.com (M. Yan), chensuhong@aliyun.com (S. Chen), zjtcmlgy@163.com (G. Lv).
[1] Hengpu Zhou, Yingjie Dong, Zhangyun Wu have contributed equally to this work.

https://doi.org/10.1016/j.ultsonch.2025.107248
Received 25 November 2024; Received in revised form 4 January 2025; Accepted 25 January 2025
Available online 1 February 2025

inflammation by improving the ratio of T-lymphocyte subpopulations and B-lymphocytes and regulating the balance of Th17/Treg[10,11].

Plant polysaccharides have a strong affinity for water molecules, and most polysaccharides have a high solubility in water and increase in solubility with increasing temperature within a certain range, so the most common extraction method for polysaccharides is hot water extraction[12,13]. Hot water extraction method is widely used in industrialized polysaccharide extraction because of its simple operation and low cost, but too high temperature may lead to the destruction of polysaccharide results. Ultrasonic extraction method through the mechanical effect of ultrasound, cavitation effect and thermal effect can effectively destroy the plant cell wall, accelerate the dissolution of active ingredients in plant cells, can effectively extract polysaccharide extraction efficiency, but need to control the ultrasound time, to avoid the degradation of soluble polysaccharides[14,15]. The principle of ultrasonic extraction of polysaccharides involves the mechanical and thermal effects of ultrasound. The mechanical effect can enhance solvent penetration into the herb's surface and accelerate the dissolution of active components. Additionally, the solubility of active components is increased through the thermal effect produced by the ultrasonic process. Under the action of ultrasound, polysaccharide particles undergo intense vibrations, leading to the rupture of cell walls and membranes, thereby releasing polysaccharide molecules. Ultrasound can also induce molecular movement and vibration in the liquid, increasing the mass transfer rate between the solvent and the sample, thereby accelerating the dissolution and diffusion of polysaccharides. Studies have shown that the ultrasonic-assisted extraction process of DOP conforms to Fick's second law. The increase in ultrasonic intensity accelerates the processes of solvent penetration, internal diffusion, and external diffusion, thereby enhancing the swelling rate of Dendrobium Officinale particles. Enzymatic extraction method is the use of one or more enzyme specificity, through the enzyme at a lower temperature to decompose the plant cell wall, cellulose and pectin are the main components of plant cell wall, so cellulase and protease are common enzymatic hydrolysate[16,17]. Enzymatic extraction rate is high and conditions are mild, but there are problems such as complex operation and high price. There is also microwave-assisted extraction, supercritical fluid extraction, low eutectic solvent extraction method or a combination of multiple methods to assist extraction. Ultrasound-assisted enzymatic extraction of polysaccharides is commonly used in research, which can effectively reduce the cost and significantly increase the yield of polysaccharides [18,19]. Due to the high polysaccharide content and sticky nature of Dendrobium Officinale, traditional high-temperature water extraction methods require extensive crushing or grinding, large amounts of water, and repeated long-duration extraction processes to achieve complete extraction. The viscosity of DOP during extraction also affects the subsequent release of polysaccharides, often leading to incomplete extraction and resource wastage. Therefore, exploring more efficient methods for DOP extraction is crucial. Ultrasound-assisted enzymatic extraction leverages ultrasound to disrupt cells, combined with enzymatic hydrolysis to facilitate the diffusion and release of polysaccharides. This method not only enhances extraction efficiency but also helps mitigate the structural damage to polysaccharides to a certain extent. Hence, we opted for ultrasound-assisted enzymatic extraction to extract DOP.

In this experiment, the ultrasound-assisted enzymatic extraction of DOP was studied in depth, firstly, a single factor was used to screen out the factors that had a greater influence on the extraction of polysaccharide yield, and then GA-BP was used to carry out response surface experiments, and then the optimal extraction process was fitted by the software, and the polysaccharides of DOP obtained under the optimal process were characterized. Finally, the immunocompromised model mice were used to evaluate the immune-enhancing effect of the polysaccharides of DOP. It provides the basis for the subsequent development of DO polysaccharide products.

2. Materials and methods

2.1. Materials and chemicals

The Dendrobium Officinale used in the experiments was identified as the dried stem of Dendrobium Officinale Kimura & Migo by Xiaona Yu (Chief Pharmacist of Chinese Medicine at Shaoxing Central Hospital), and purchased from Zhejiang Yunzhitang Biotechnology Co., LTD. Cellulase (50 U/mg) was purchased from Shanghai Yuanye Biotechnology Co., LTD (Shanghai, China). IgA, IgG, IL-1, IL-6, and IL-10 ELISA kits were purchased from Jiangsu Meimian Industrial Co., LTD (Jiangsu, China). $CD3^+$, $CD4^+$, $CD8^+$ antibodies were purchased from Multisciences (LianKe) Biotech, CO., LTD (Zhejiang, China). Reference standards were purchased from Chengdu Pufei De Biotech CO., LTD (Sichuan, China). CD4, CD8 antibody were purchased from Daige Biotechnology Co., Ltd (Zhejiang, China). All the additional chemicals were of analytical quality or above, and all water used for separation and examination was filtered and deionized.

2.2. DOP extraction process optimization

2.2.1. Extraction process

4 g of Dendrobium Officinale was weighed precisely, water and cellulase were added, the mixture was subjected to ultrasonic treatment at different temperatures. After ultrasonication, heat in boiling water bath for 10 min, extract and filter, concentrate to 100 mL under reduced pressure. 400 mL of anhydrous ethanol was slowly added to the extract, and it was left at 4 °C overnight, centrifuged at 3500 r/min for 10 min, the precipitate was collected, and the precipitate was freeze-dried for 48 h, which was obtained as DOP.

2.2.2. Single factor experiment

Fixed conditions: at solvent dosage of 1:40, enzyme dosage of 1500 U/g, extraction temperature of 50 °C, ultrasonic extraction for 90 min, pH of 5.5. Different levels were set to investigate the effects of solvent amount, enzyme dosage, extraction temperature, extraction time and pH on the yield of DOP.

2.2.3. Response surface methodology test

Response surface optimization was carried out on the basis of one-way experiment with extraction time (X1), extraction temperature (X2), solvent dosage (X3), enzyme dosage (X4) as independent variables and DOP yield as the quantity examined (Y). The polysaccharide extraction process was optimized using Genetic Algorithm-Back Propagation (GA-BP), method is described with reference to review literature [20].

2.2.4. Polysaccharide content determination

Preparation of standard curve: weigh 10.43 mg of glucose standard in 100 mL volumetric flask, add water to form 0.1043 mg/mL of control solution. In a 10 mL stoppered test tube, take 0.1, 0.2, 0.4, 0.6, 0.8, 1.0, 1.2 mL of the control solution, and then add water to make up to 2.0 mL. Precisely add 1.0 mL of freshly configured 5 % phenol solution, mix well and then put it into an ice bath to add 5.0 mL of concentrated sulfuric acid, shake well and cool it down for 5 min, then set it into a boiling water bath for 20 min, then take it out and cool it down in an ice bath for 5 min, using the corresponding reagents as blanks. The absorbance was measured at 488 nm with the corresponding reagent as blank. The absorbance was measured at 488 nm. The concentration of glucose standard was taken as the horizontal coordinate and the absorbance as the vertical coordinate to draw the standard curve, $y = 58.9829\ x + 0.0341$, $r = 0.9995$.

Preparation of test material: In a 10 mL stoppered test tube, take 1.0 mL of test solution, add 1 mL of pure water and mix well. Add 5 % phenol solution 1.0 mL, mix well, and then placed in an ice bath add 5.0 mL of concentrated sulfuric acid, shaking well, cooling for five minutes,

placed in a boiling water bath for 20 min, removed to the ice bath cooling for 5 min, the absorbance was measured at 488 nm.

2.3. DOP characterization

2.3.1. DOP purification

After DOP was dissolved with water, it was decolorized and deproteinized to obtain the purified polysaccharide DOP.

2.3.2. Determination of polysaccharide content in DOP

The polysaccharide content of DOP was determined with reference to the previous part of the method.

2.3.3. Determination of DOP monosaccharide composition

The monosaccharide composition was determined by high performance liquid chromatography (HPLC). Dissolve 50 mg of DOP with 50 mL of water, remove 1 mL and add 500 μL of 3 mol/L HCl solution, hydrolyze at 110 °C for 1 h. After cooling, add 3 mol/L NaOH to adjust to pH = 7. Take 400 μL of the solution, add 400 μL of 0.3 mol/L NaOH and 250 μL of 0.5 mol/L PMP methanol, and mix well. Mix well, derivatize at 70 °C for 100 min, take out and let cool, then add 450 μL of 0.3 mol/L HCl solution, vortex and mix well. Then add 2 mL of trichloromethane, mix well, centrifuge, discard the trichloromethane layer, repeat the operation 4 times, and finally take the aqueous layer as the test solution.

Chromatographic conditions: Agilent 1200 liquid chromatograph (Agilent Technologies, Beijing, China), Aglient XB-C18 column (4 × 250 mm), acetonitrile (A)-0.1 mol/L ammonium acetate (B), mobile phase gradient: 0–18 min, 16.8–12 %A; 18–18.2 min, 12 %A; 18.2–22 min, 12–22 %A; 22–23 min, 22 %A; 23–25 min, 22–20 %A; 25–26 min, 20 % A; 26–42 min, 20–30 %A; 42–60 min, 30 %A. flow rate 1.0 ml/min, 30 ℃, injection volume 5 μL, 250 nm.

2.3.4. DOP electron microscope scanning

After taking an appropriate amount of DOP samples on the conductive adhesive for sticking table and spraying gold, the surface micromorphology and structure of the polysaccharide samples were observed by Motic Desktop Scanning Electron Microscope (McAudi Industrial Group Co., Ltd., Fujian, China) under different magnifications and voltages.

2.3.5. Congo red test

Weigh 5 mg DOP, add 2.0 mL of distilled water and 2.0 mL 80 μmol/L of Congo red reagent, and gradually add 1.0 mol/L of NaOH solution, so that the final concentration of NaOH in the solution was gradually increased from 0.0 mol/L to 0.5 mol/L, and scanned with UV–visible recording spectrometer, and the maximum absorption wavelengths were measured for each NaOH concentration condition.

2.3.6. Molecular weight determination

High performance gel permeation chromatography (HPGPC) was used to determine the molecular weight and purity of DOP.

Preparation of test material: 5 mg of each sample was weighed and dissolved in 1 mL of mobile phase solution to form 5 mg/mL solution, vortexed and dissolved, and then centrifuged at 12000 rpm for 10 min. The supernatant was aspirated and filtered through 0.22 μm aqueous microporous filter membrane, and then the sample was transferred to a 1.8 mL injection vial.

Chromatographic conditions: 0.05 M NaCl solution; Column: BRT105-103–101 (8 × 300 mm); Flow rate: 0.7 mL/min; Column temperature: 40 °C; Injection volume: 25 μL; Detector: Differential detection RID-20A.

2.4. Study on the immunomodulatory effects of DOP

2.4.1. Experimental design

Twenty-four male ICR mice (6–8 weeks old) were randomly divided into 4 groups (6 mice in each group) according to body weight: the normal group (NC), the model group (MC), the DOP low dose group (DOP-L, 50 mg/kg), the DOP high dose group (DOP-H, 200 mg/kg). Cyclophosphamide 80 mg/kg was injected intraperitoneally daily in the model group and the administered group for 3 consecutive days, and starting from the 4th day, DOP was gavaged in the administered group, and an equal amount of pure water was gavaged in the normal group and the model group for 15 consecutive days. The animals were acclimatized for seven days to conditions of 23 ± 2°C, 55 ± 5 % humidity, a 12 h light/dark cycle, and a well-ventilated environment, with free access to food and water. This study received approval from the Ethics Committee of Zhejiang Chinese Medical University (20240418–27).

2.4.2. Behavioral measurements

On the 14th day, grip strength, weight-bearing swimming time, and number of voluntary activities were measured, and the body weights of mice were determined at 0th, 5th, 10th, and 15th day of administration.

2.4.3. Macrophage phagocytosis assay

Four days before the experiment, each mouse was injected intraperitoneally with 0.2 mL of 2 % sheep blood erythrocytes. Mice were injected intraperitoneally with 4 mL of Hank's solution with calf serum, and the abdomen was gently kneaded for 20 times to wash out the peritoneal macrophages, and then the abdominal wall was cut open, and the abdominal lavage solution was sucked up by 2 mL of a rubber-tip pipette into a test tube. Use a 1 mL sampler to draw up 0.5 mL of peritoneal lavage fluid and add it to 0.5 mL of 1 % chicken blood erythrocyte suspension in a test tube, and mix well. Use a syringe to aspirate 0.5 mL of the mixture and add it to the agar ring of the slide. Incubate in an incubator at 37 °C for 15–20 min. At the end of incubation, quickly rinse off the unaffixed cells with saline, fix them in methanol solution for 1 min, and stain with Giemsa solution for 15 min. The cells were rinsed with distilled water, dried, and observed under a microscope, and the phagocytosis rate and phagocytic index were counted.

2.4.4. ELISA

Blood was collected from mice after anesthesia, serum was separated, and IgA, IgG, IL-1, IL-6, and IL-10 levels in serum were determined according to the method in the ELISA kit.

2.4.5. Flow cytometry

Take 50 μL of mouse blood, add 2 μL of $CD3^+$, $CD4^+$, $CD8^+$ antibody, incubate for 15 min and then add erythrocyte lysate to lysed for 10 min, centrifuge to take the supernatant, and use flow cytometer (Beckman, USA) to detect cell typing.

2.4.6. Organ coefficient

Mice were rapidly isolated from the spleen and thymus after execution, weighed, and organ coefficients were calculated.

2.4.7. Hematoxylin-Eosin (HE) Staining

After the last administration, the mice were fasted without water for 24 h, anesthetized and executed, and the spleen tissues were quickly dissected and taken from the mice, washed with saline and put into a bottle containing 10 % neutral formalin buffer. After fixation, extraction, dehydration, embedding and sectioning, 4 μm paraffin sections were prepared, stained with hematoxylin-eosin HE, sealed with neutral resin, and then dried under the microscope to observe the histopathological changes of the spleen.

2.4.8. Western Blotting (WB)

Spleen tissue was taken, fully ground with liquid nitrogen, added appropriate amount of RIPA lysate, left on ice for 10 min, centrifuged and supernatant was taken, and tissue protein was extracted. Protein concentration was determined by BCA method, protein samples were subjected to sodium dodecyl sulphate–polyacrylamide gel

electrophoresis, transferred to PVDF membrane, enclosed in 5 % BSA for 1.5 h, CD4 and CD8 antibodies were added respectively, and the samples were incubated at 4 °C for overnight, and then washed three times by TBST. The membrane was washed three times, each time for 15 min, the secondary antibody was added, incubated at room temperature for 2 h, the membrane was washed three times, each time for 15 min, and ECL chemiluminescent solution was added, then the protein bands were detected by gel imager and analyzed by Image-J software.

3. Results and discussion

3.1. DOP extraction process optimization results

3.1.1. DOP single factor experiment results

The effects of different factors on polysaccharide yield are shown in Fig. 1. The extraction temperature showed a trend of increasing and then decreasing polysaccharide yield as the temperature increased. The optimum temperature for cellulase activity is 40–60 °C, and the enzyme may decompose after exceeding 60 °C, while the enzyme activity is not good below 40 °C.

Extraction time, material-liquid ratio, and enzyme addition showed the same trend, with a significant increase and then flattening. pH in the range of 4–6 had little effect on the polysaccharide extraction rate, so pH was not examined subsequently.

The highest level of polysaccharide yield and the level before and after each factor were selected, such as extraction time of 60, 90, 120 min; extraction temperature of 40, 50, 60 °C; material-liquid ratio of 40, 60, 80; and enzyme addition of 1000, 1500, 2000 for the subsequent GA-BP experiments.

3.1.2. GA-BP optimization results

GA-BP model, as an intelligent system that simulates the organizational structure of human brain and helps to deal with the preferred algorithm of nonlinear relationship, has been successfully applied in the fields of Chinese medicine preparation research, Chinese medicine diagnosis, and Chinese medicine ingredient content prediction[20,21]. A large number of studies have confirmed that the GA-BP model can find the optimal conditions in a wide range through autonomous learning with fewer experiments and less research time and effort[22], and is suitable for multifactorial tests of Chinese medicine extraction.

The GA-BP results are shown in Table 1, the thresholds and weights were optimized by the genetic algorithm to construct the GA-BP neural network, in which the number of neurons in the input layer was 4 (material-liquid ratio, extraction time, extraction temperature, and enzyme additive); the number of neurons in the output layer was 1 (polysaccharide yield); and the number of neurons in the hidden layer was set to 3. First, the parameters of the genetic algorithm were initialized, the initial population size was set to 30, the maximum number of iterations was set to 50, the crossover probability was set to 0.8, and the variance probability was set to 0.2. The relationship between each generation and the fitness value was calculated, as shown in Fig. 2A. The optimal fitness value is 2.09, and the average fitness value is 7.03. Through population selection, crossover and mutation, the weights and thresholds are continuously updated, and finally the weights and thresholds that satisfy the convergence conditions are obtained. The network training parameter values were set, the number of training sessions was 1000, the minimum error of the training objective was set to 0.00001, and the neural network was evaluated by the mean square error value (MSE). Fig. 2B shows the performance of the training and test sets for different number of periods. The optimal extraction process conditions were: extraction time 102 min, extraction temperature 48 degrees, material-liquid ratio 80, enzyme addition 1600 U/g, and predicted polysaccharide yield 29.64 %. Three extractions were carried out according to the optimal extraction process for validation and the polysaccharide yield was 29.78 %, 29.97 % and 29.37 %, respectively.

3.2. DOP characterization

3.2.1. Polysaccharide characterization

Scanning electron microscope utilizes a high-energy electron beam to interact with the polysaccharide indication to generate signals, and

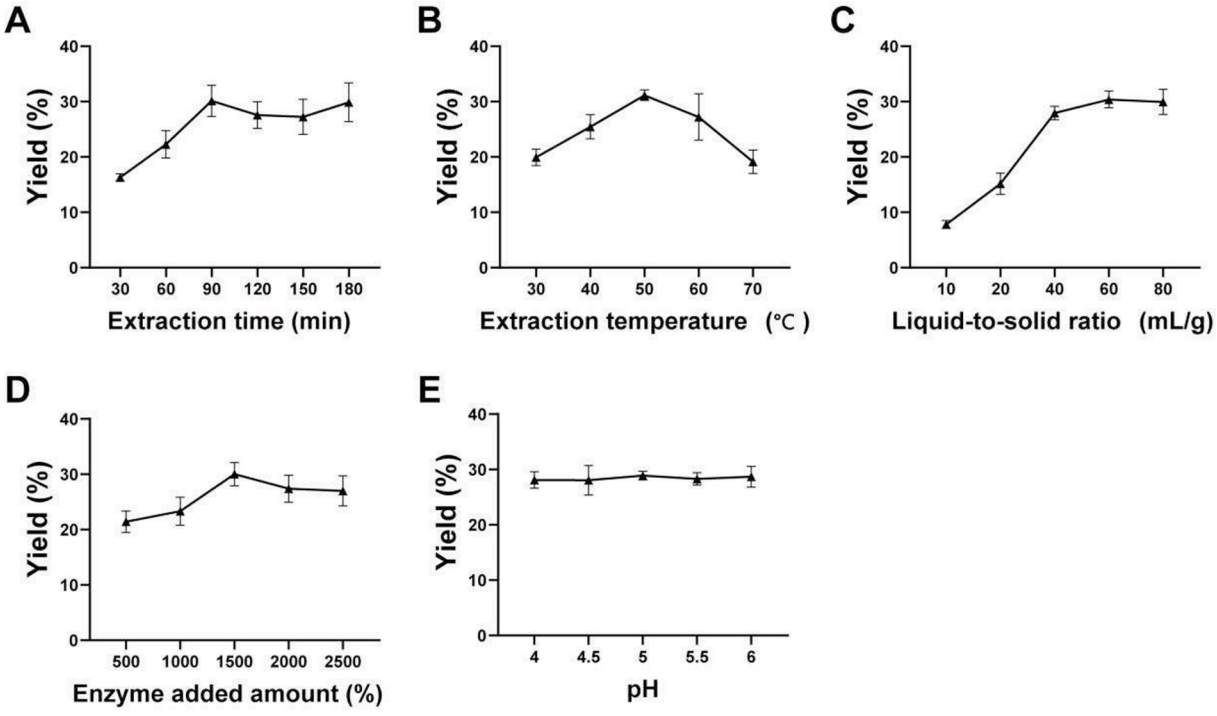

Fig.1. Effects of different factors and levels on polysaccharide yield. A, Extraction time; B, Extraction temperature; C. Liquid-to-soild ratio; D, Enzyme added amount; E, pH.

Table 1
Response surface experimental design and results.

Runs	Extraction time (min)	Extraction temperature (°C)	Liquid-to-solid ratio (mL/g)	Enzyme added amount (U/g)	Yield (%) Actual	GA-BP Predicted
1	0 (90)	−1 (40)	1 (80)	0 (1500)	31.73	29.63
2	0 (90)	−1 (40)	0 (60)	1 (2000)	31.85	29.63
3	−1 (60)	0 (50)	0 (60)	1 (2000)	26.92	23.34
4	1 (120)	−1 (40)	0 (60)	0 (1500)	30.23	29.61
5	1 (120)	0 (50)	0 (60)	1 (2000)	28.81	29.54
6	−1 (60)	0 (50)	1 (80)	0 (1500)	22.91	23.34
7	0 (90)	0 (50)	−1 (40)	1 (2000)	24.56	23.34
8	−1 (60)	0 (50)	0 (60)	−1 (1000)	30.01	29.58
9	0 (90)	−1 (40)	−1 (40)	0 (1500)	29.75	29.63
10	0 (90)	−1 (40)	0 (60)	−1 (1000)	23.13	24.67
11	−1 (60)	1 (60)	0 (60)	0 (1500)	22.45	23.34
12	0 (90)	0 (50)	1 (80)	1 (2000)	22.87	23.34
13	0 (90)	1 (60)	1 (80)	0 (1500)	23.04	23.34
14	1 (120)	0 (50)	0 (60)	−1 (1000)	28.82	24.68
15	−1 (60)	0 (50)	−1 (40)	0 (1500)	22.92	23.34
16	0 (90)	1 (60)	−1 (40)	0 (1500)	23.82	23.34
17	0 (90)	0 (50)	0 (60)	0 (1500)	30.08	29.62
18	0 (90)	0 (50)	0 (60)	0 (1500)	29.99	29.62
19	0 (90)	0 (50)	0 (60)	0 (1500)	30.27	29.62
20	1 (120)	0 (50)	−1 (40)	0 (1500)	31.50	29.64
21	0 (90)	0 (50)	0 (60)	0 (1500)	31.02	29.62
22	−1 (60)	−1 (40)	0 (60)	0 (1500)	27.04	29.63
23	0 (90)	1 (60)	0 (60)	−1 (1000)	24.61	23.35
24	1 (120)	0 (50)	1 (80)	0 (1500)	32.21	29.64
25	0 (90)	1 (60)	0 (60)	1 (2000)	22.35	23.34
26	0 (90)	0 (50)	−1 (40)	−1 (1000)	22.75	24.69
27	0 (90)	0 (50)	0 (60)	0 (1500)	29.63	29.62
28	1 (120)	1 (60)	0 (60)	0 (1500)	22.42	23.35
29	0 (90)	0 (50)	1 (80)	−1 (1000)	24.01	24.69

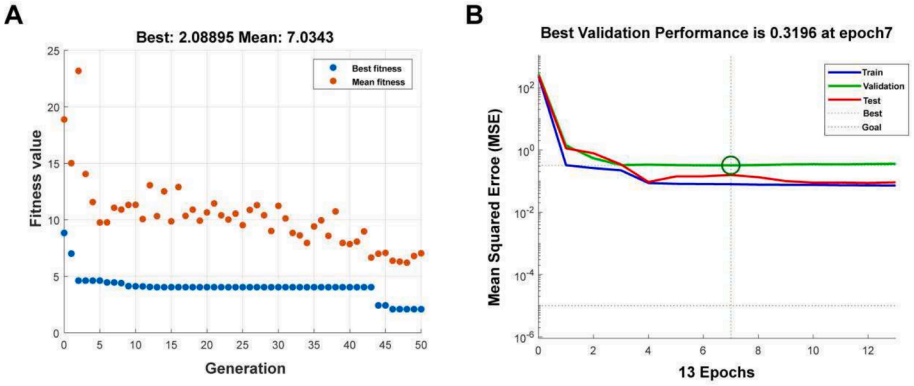

Fig. 2. The performance of the GA-BP model. A, fitness function plot of GA-BP neural network; B, GA-BP neural network MSE for different data sets.

obtains high-resolution polysaccharide morphology images through computer processing, which is used to observe the spatial distribution and allotropic combinations of polysaccharide molecules. DOP was observed to be reticulate under the electron microscope, and a large number of irregular cavities were visible in DOP polysaccharides after the method 10,000 times. The elemental composition of DOP was scanned and found to contain 55.14 % carbon and 43.91 % oxygen, respectively (Fig. 3A).

3.2.2. Polysaccharide content and composition

The polysaccharide content of DOP was determined by UV–Vis and the polysaccharide content of DOP was 90.66 ± 2.47 %. The composition of DOP monosaccharides was determined using HPLC pre-column derivatization, and the results showed that DOP was mainly composed of mannose, glucose, galactose, and arabinose, with a molar ratio of 74.17: 47.80: 9.03: 1. (Fig. 3B). Different extraction methods disrupt the plant cell wall to different degrees, which in turn leads to different composition and chemical structure of the soluble, such as Liu[23] used hot water extraction-ethanol precipitation method to obtain the composition of DOP as Man: Glc = 3.45:1; whereas the polysaccharides obtained from DOP by Guo[24] using ultrasound-assisted hot water extraction were composed of Man, Glc, Ara, and Gal, with a molar ratio of 50.89:30.17:4.78:1. It is evident that different extraction methods have a greater effect on the composition and ratio of monosaccharides in DOP.

3.2.3. Congo red test results

The reaction between Congo red and polysaccharide with triple-helix structure will form a complex, which is its maximum absorption wavelength redshifted, but after the NaOH concentration exceeds a certain range, the complex will be hydrolyzed, and the maximum absorption wavelength decreases[25,26]. As seen in Fig. 3C, the maximum absorption wavelength of DOP mixed with Congo red solution did not change significantly with the increase of NaOH concentration, and it was hypothesized that the three-stranded helical structure might not exist in DOP.

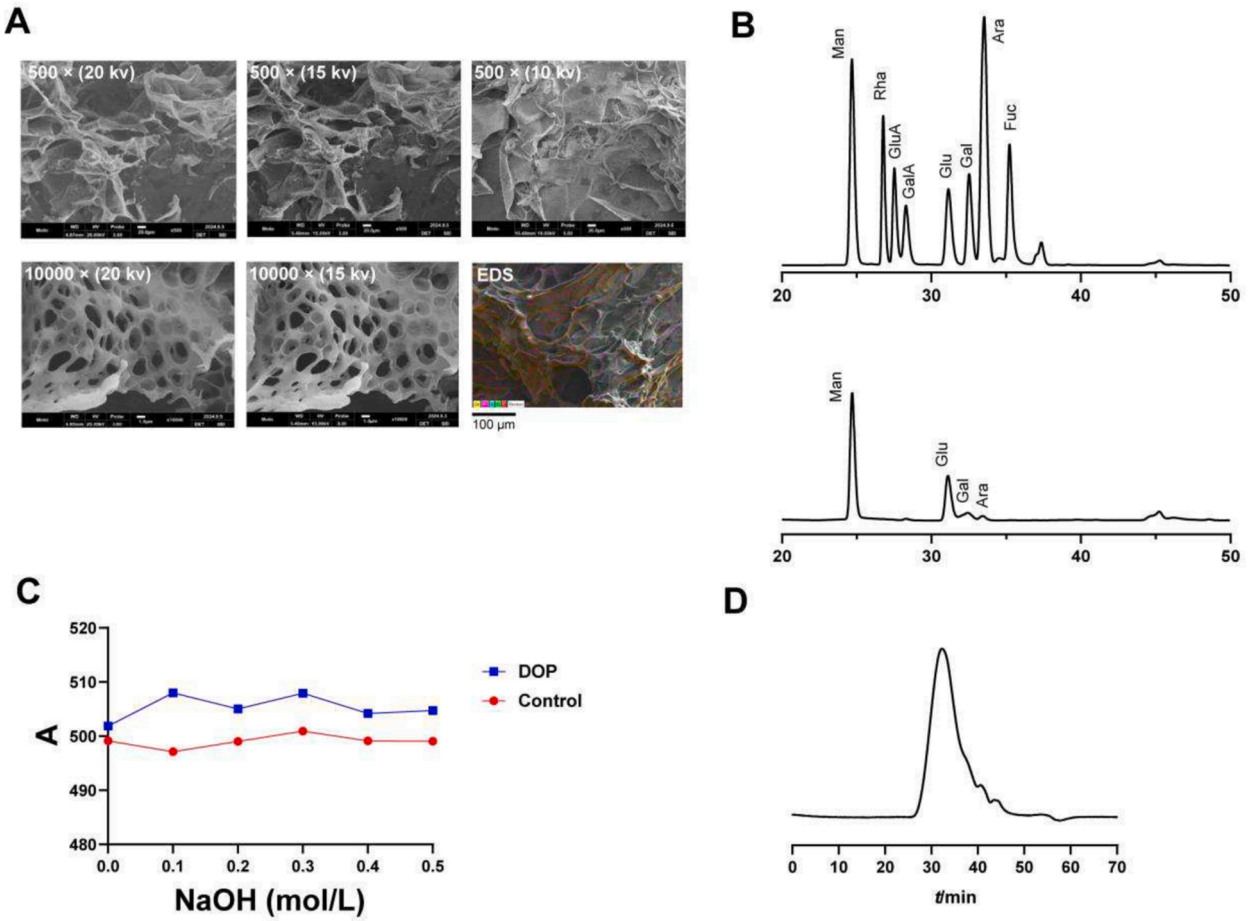

Fig. 3. DOP characterization. A, SEM; B, monosaccharide composition; C, Congo red; D, molecular weight. (For interpretation of the references to colour in this figure legend, the reader is referred to the web version of this article.)

3.2.4. *Molecular weight*

The effect of molecular weight on the biological activity of polysaccharides is important for the development and production preparation of active polysaccharides; higher molecular weights of polysaccharides result in poorer water solubility and higher solution viscosity, but it is the suitably high molecular weights that may lead to the formation of effective active structures[27,28]. We determined the molecular weight and purity of DOP by HPGPC. A standard curve: $y = -0.2052x + 11.9710$ was fitted based on the molecular weight of dextran standards, $r = 0.9976$. DOP molecular mass was heterogeneous, and the relative molecular weight of the main component was 2.20×10^6 Da with a retention time of 32.305 min, which accounted for 81.317 % (Fig. 3D). The molecular weight of DOP we obtained was large, and we found that the polysaccharide could not be completely solubilized after the drug concentration was greater than 20 mg/mL and the viscosity was high in the later animal experiments during the formulation process, so we chose 200 mg/kg as the high dose.

3.3. *DOP ameliorates cyclophosphamide-induced immunodeficiency in mice*

3.3.1. *DOP improves general signs in immunocompromised mice*

Cyclophosphamide acts as an antitumor agent as well as a cytotoxic immunosuppressant, which has a strong and long-lasting immunosuppressive effect [29,30]. In our experiments, the body weight of mice in the model group increased slowly during the administration of the DOP, and a significant difference between the body weight of the model group and that of the normal group appeared on the 10th day ($P < 0.01$); On the 15th day of the administration of the DOP, the body weights of all groups increased significantly compared with those of the model group ($P < 0.05$ or 0.01, Fig. 4A and B).

In addition, the results of grip strength and weight-bearing swimming experiments showed that grip strength and swimming time were significantly increased in both normal and DOP groups compared with the model ($P < 0.05$ or 0.01, Fig. 4C and D). This suggests that cyclophosphamide affects the developmental and physical performance of the mice, whereas DOP intervention can reverse the above adverse effects.

3.3.2. *DOP improves blood indices in immunocompromised mice*

Lymphocytes, a type of white blood cell, are produced by lymphoid organs and are the primary performers of almost all immune functions of the lymphatic system[31]. Leukocytes have the ability to phagocytose foreign substances and produce antibodies against invading pathogens [32]. Cyclophosphamide belongs to the cell cycle non-specific chemotherapeutic drugs, which have killing effects on all cells in the proliferation cycle. The blood routine results showed that the model group of mice had significantly fewer leukocytes and lymphocytes than the normal group, and the DOP administration intervention group had significantly more leukocytes and lymphocytes than the model group ($P < 0.05$ or 0.01, Fig. 4E).

3.3.3. *DOP regulates cytokines in immunocompromised mice*

Immunoglobulins are a class of proteins with antibody activity in human serum and body fluids. It has antibacterial and antiviral effects and enhances phagocytosis of cells, and can kill or dissolve pathogenic microorganisms under the synergy of complement[33,34]. The serum levels of IgA and IgG in the model group of mice were significantly lower than those in the normal group, whereas DOP significantly improved

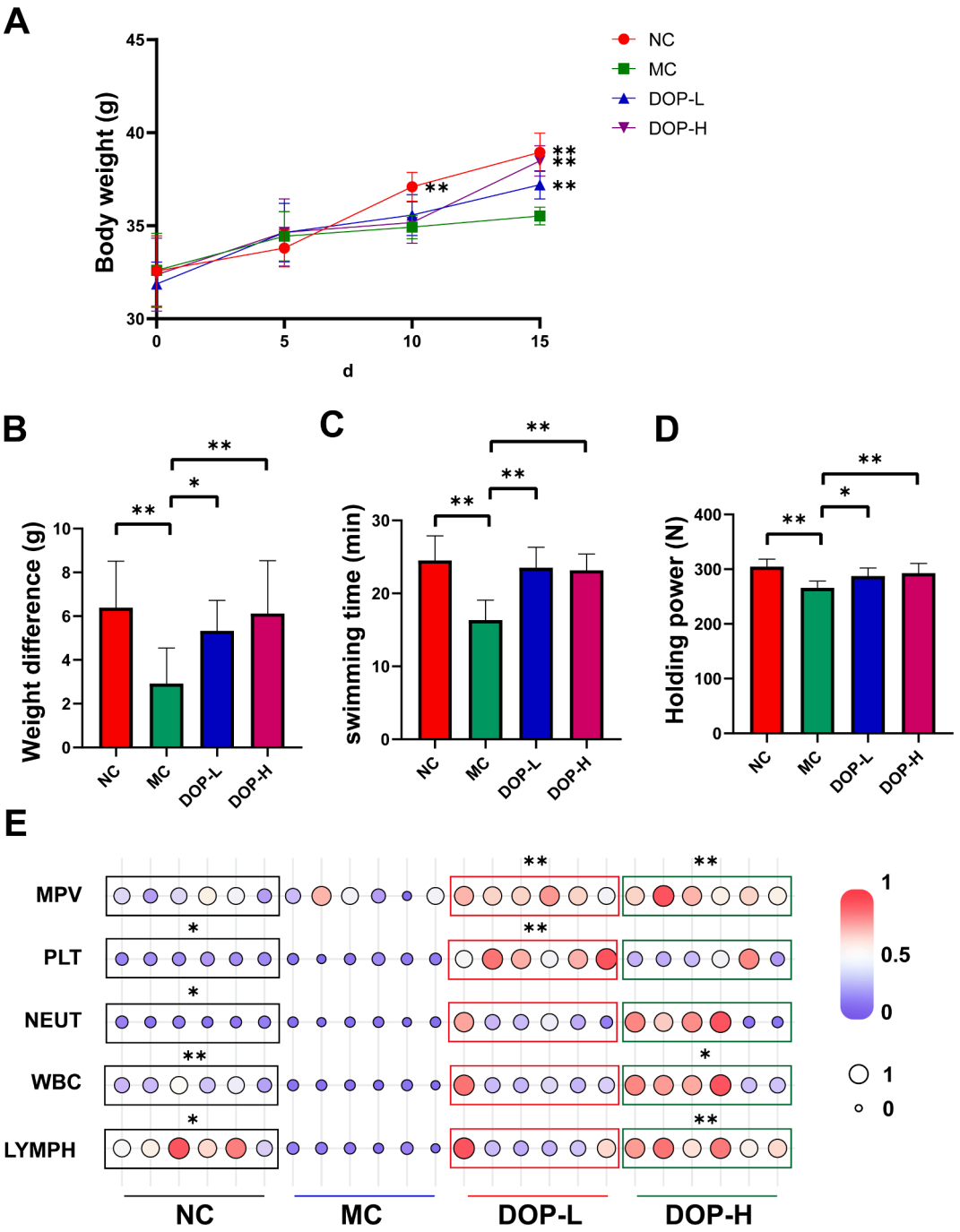

Fig. 4. Effects of DOP on general signs and blood routine of immunocompromised mice. A, body weight; B, weight difference; C, swimming time; D, holding power; E, blood routine examination. N = 6, compared with MC, *$P < 0.05$, **$P < 0.01$. NC, the normal group; MC, the model group; DOP-L, the DOP low dose group; DOP-H, the DOP high dose group.

them ($P < 0.05$ or 0.01, Fig. 5A and B).

IL-1 and IL-6 are involved in inflammation and immune regulation, and their elevated levels often represent increased inflammation and decreased immunity in the body[35,36]; whereas IL-10 is thought to be a key produced by many different types of immune cells and tissue epithelial cells anti-inflammatory cytokine and elevated levels can serve to enhance immunity[37]. Serum levels of IL-1 and IL-6 were significantly elevated and IL-10 levels were significantly decreased in the model group of mice; IL-10 levels were significantly increased in the administered group compared to the model group ($P < 0.05$ or 0.01, Fig. 5C-E).

3.3.4. *DOP regulates T-lymphocyte subpopulations in immunocompromised mice*

Measurement of T-lymphocyte subsets is an important indicator of the body's cellular immune function $CD4^+$ T-cells are a subpopulation of lymphocytes produced by the thymus and play an important role in the immune response[38]. Especially in cell-mediated immunity, $CD4^+$ T cells mainly recognize and respond to foreign antigens presented by antigen-presenting cells. This response regulates the activity of other immune cells, such as B cells or $CD8^+$ T cells, and can also initiate a new immune response[39]. $CD8^+$ T can suppress both humoral and cellular immunity by direct and indirect means, including the secretion of inhibitory cytokines, granzymes, and perforins, etc., and indirectly, by

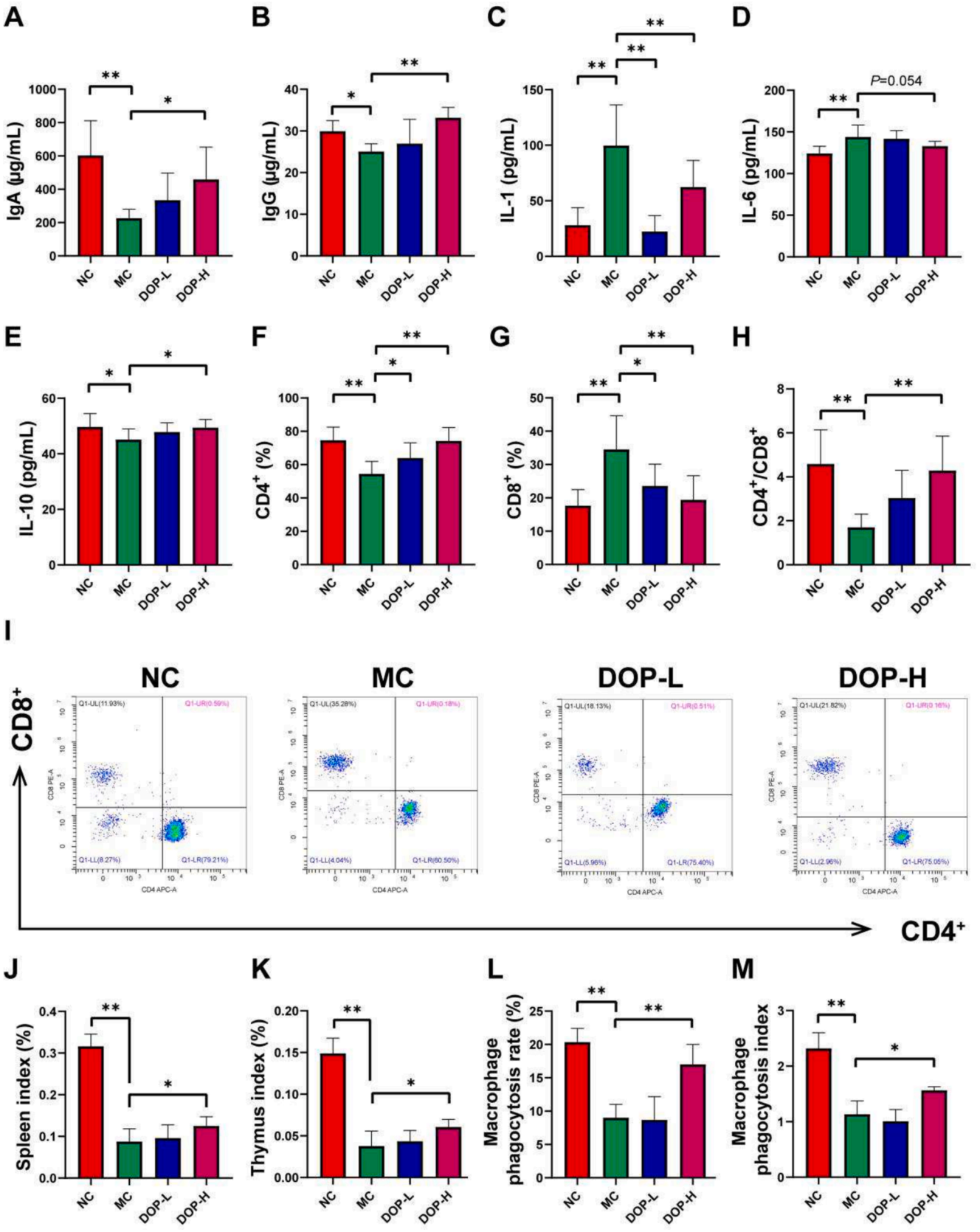

Fig. 5. Effect of DOP on immune function. A, IgA; B, IgG; C, IL-1; D, IL-6; E, IL-10; F, $CD4^+$; G, $CD8^+$; H, $CD4^+/CD8^+$; I, representation picture of flow cytometry; J, spleen index; K, thymus index; L, macrophage phagocytosis rate; M, macrophage phagocytosis index. N = 6, compared with MC, $^*P < 0.05$, $^{**}P < 0.01$. NC, the normal group; MC, the model group; DOP-L, the DOP low dose group; DOP-H, the DOP high dose group.

facilitating the conversion of DCs to double-positive DCs for tolerogenic immunoglobulin-like transcripts.

Dysregulation of $CD4^+$ ratio and $CD4^+/CD8^+$ balance was commonly seen in patients with malignant tumors, immunodeficiency diseases, or who were on immunosuppressive drugs, and the use of cyclophosphamide resulted in dysregulation of $CD4^+/CD8^+$ ratio[40–42]. Compared with the normal group, the model group showed a significant increase in the $CD8^+$ ratio and a significant decrease in the $CD4^+$ and $CD4^+/CD8^+$ ratios ($P < 0.01$). Compared with the model group, mice in the DOP group had a significantly lower $CD8^+$ ratio and significantly higher $CD4^+$ and $CD4^+/CD8^+$ ratios ($P < 0.05$ or 0.01, Fig. 5F-I).

3.3.5. *DOP improves spleen and thymus structure and function in immunocompromised mice*

The thymus is the site of differentiation, development and maturation of T cells, which develop from hematopoietic stem cells and enter the thymus from the circulation and are stimulated by thymic epithelial cells to differentiate into T cells[43]. The spleen is the largest and most efficient immune organ in the body, with the main cellular components being B lymphocytes, T lymphocytes, macrophages, etc[44]. The spleen contains 25 % of the systemic circulating T cells. Containing 25 % of systemic circulating T-lymphocytes and most of the macrophages, the spleen contains a large number of immunoreactive cells and their mediated immune factors, which play an important role in the regulation of immunity. Compared with the normal group, the spleen and thymus indices of mice in the model group were significantly decreased ($P < 0.01$); compared with the model group, the spleen and thymus indices of mice in the DOP group were significantly increased ($P < 0.05$, Fig. 5J and K).

Macrophages has the functions of phagocytosis, elimination of intracellular parasitic bacteria and fungi, and removal of senescent self-cells. When pathogens or other foreign bodies invade the organism, macrophages take the initiative to approach to the foreign body, endocytose as cytoplasm to form phagocytosis, and kill the pathogens and digest and decompose them under the action of lysosomal enzymes [45,46]. We determined the ability of macrophages to phagocytose chicken erythrocytes, and found that the macrophage phagocytosis rate and phagocytosis coefficient of mice in the model group were significantly lower compared with the normal group ($P < 0.01$); the macrophage phagocytosis rate and phagocytosis coefficient of mice in the DOP group were significantly increased compared with the model group ($P < 0.05$ or 0.01 Fig. 5L and M).

In the normal group, the spleen was structurally complete, with clear boundaries between the red and white medullas, and lymphocytes were closely arranged in the lymph nodes of the white medulla. In the model group, the boundaries between the red and white medullas of the spleen

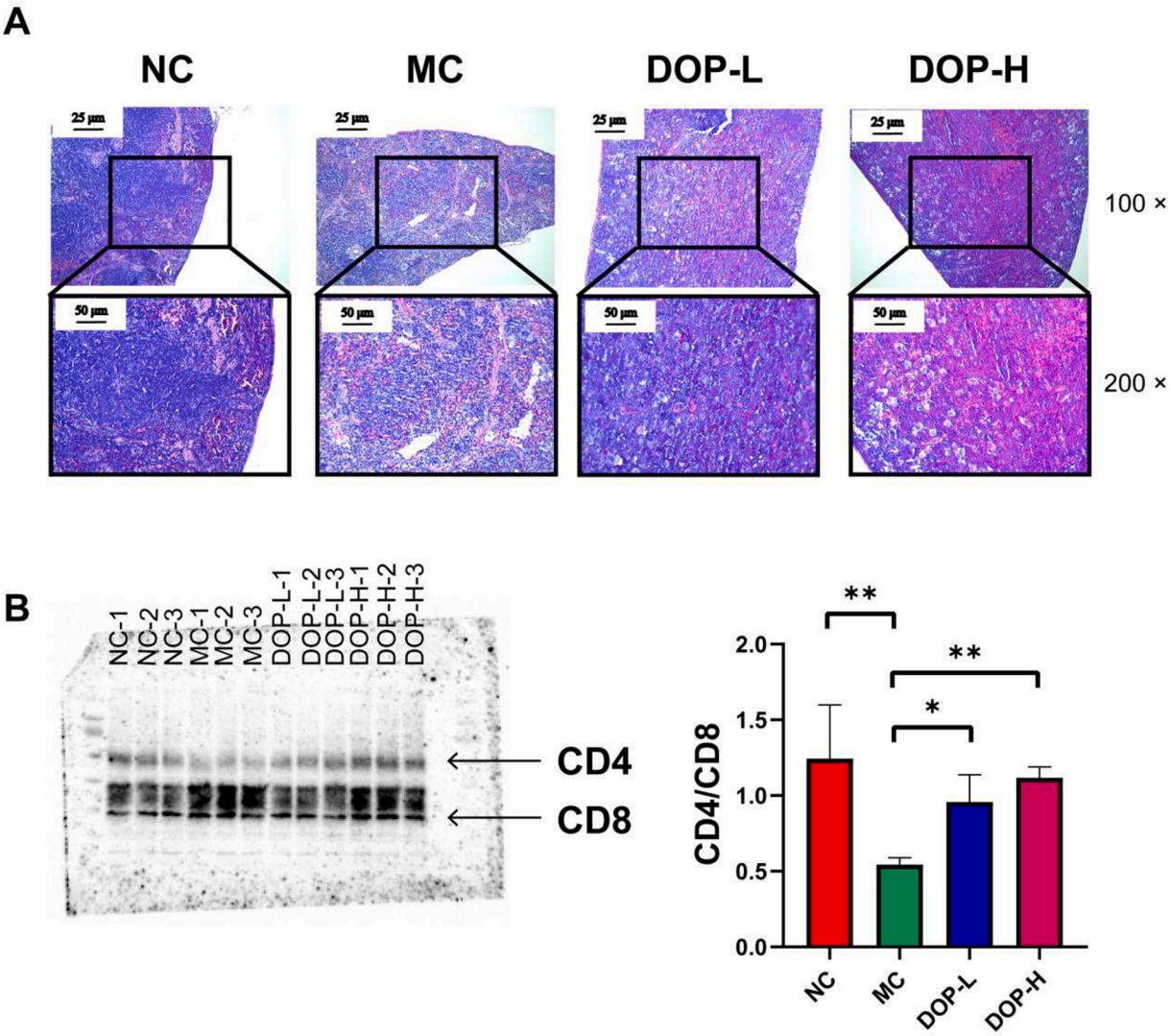

Fig. 6. Effects of DOP on splenic morphology and CD4/CD8 protein expression in spleen. A, splenic morphology (100 × and 200 ×); B, CD4/CD8 protein expression. Compared with MC, $^*P < 0.05$, $^{**}P < 0.01$. NC, the normal group; MC, the model group; DOP-L, the DOP low dose group; DOP-H, the DOP high dose group.

were blurred, the lymph nodes were loosely arranged, and the splenic microsomes were blurred in structure, atrophied, and had diluted lymphocytes. The structure and morphology of the spleen in the DOP group were more complete, and the boundaries were clearer (Fig. 6 A).

Finally, we used Western Blot to detect the protein expression of CD4/CD8 in the spleen. The WB results showed that the expression of CD4/CD8 was significantly decreased in the model group compared with the normal group; and the expression of CD4/CD8 was significantly increased in the DOP group compared with the model group. ($P < 0.05$ or 0.01, Fig. 6B).

Taken together, DOP may play an immune-enhancing role by improving thymic and splenic coefficients and pathomorphology, enhancing macrophage phagocytosis in the spleen, and upregulating CD4/CD8 protein expression.

4. Conclusion

We optimized the extraction process of Dendrobium Officinale polysaccharides (DOP) using GA-BP with ultrasound-assisted enzymatic methods. The obtained polysaccharides were characterized, and the immunomodulatory effects of DOP were preliminarily explored. The results demonstrated that the optimal conditions for DOP extraction are: an extraction time of 102 min, an extraction temperature of 48°C, a material-to-liquid ratio of 1:80, and an enzyme addition of 1600 U/g. This method predicted a polysaccharide yield of 29.64 %, with an actual yield of 29.71 ± 0.31 %. The obtained DOP was a non-pure white powder with a porous structure, containing 90.66 ± 2.47 % polysaccharides. It was mainly composed of mannose, glucose, galactose, and arabinose in the proportions of 74.17: 47.80: 9.03: 1, respectively. This study indicates that the GA-BP optimized ultrasound-assisted enzymatic extraction method is stable and reliable. Additionally, DOP improved the immune function of immunocompromised mice within 15 days, potentially by regulating T lymphocyte ratios and CD4/CD8 expression. The extraction method obtained in this experiment is stable and reliable, which can provide a reference for the development of Dendrobium Officinale polysaccharide products.

CRediT authorship contribution statement

Hengpu Zhou: Writing – review & editing, Writing – original draft, Formal analysis, Data curation, Conceptualization. **Yingjie Dong:** Project administration, Conceptualization. **Zhangyun Wu:** Writing – original draft, Data curation. **Xi Peng:** Formal analysis. **Meiqiu Yan:** Visualization, Validation, Supervision. **Suhong Chen:** Supervision. **Guiyuan Lv:** Resources, Funding acquisition.

Declaration of competing interest

The authors declare that they have no known competing financial interests or personal relationships that could have appeared to influence the work reported in this paper.

Acknowledgments

This study was supported by the National Key Research and Development Program (No. 2017YFC1702203), the Key Laboratory of Zhejiang Province (No. 2012E10002), Natural science fundation of Zhejiang province (NO. LY24H280005 and No. ZCLMS25H2801), National Natural Science Foundation of China (No. 82274134 and No. 82404900), and the China Postdoctoral Science Foundation (No. 2024M762962).

All authors disclosed no relevant relationships.

Data Availability Statement

The data presented in this study are available on request from the corresponding authors upon reasonable request.

Ethical Statement

This study was performed in accordance with the standard guidelines for the "Care and Use of Laboratory Animals" of Zhejiang Chinese Medical University and received approval from the Ethics Committee of Zhejiang Chinese Medical University (20240418-27).

References

[1] L. Lian, Z. Yanli, L. Zhimin, W. Yuanzhong, A strategy of fast evaluation for the raw material of Tiepi Fengdou using FT-NIR and ATR-FTIR spectroscopy coupled with chemometrics tools, Vibrational Spectroscopy (2022).
[2] Z. Quan, Y. Caijun, Y. Xiaoying, P. Qian-Qian, L. Jianfei, L. Mingming, W. Xuanjun, S. Jun, Dendrobium officinale Orchid Extract could improve wound healing in diabetic mice, Research Square (research Square) (2020).
[3] L. Zhengfei, L. Lian, N. Qiang, H. Mao Hsuan, L. Chunlii, S. Yedong, M. Yunxiang, Y. Jianhua, D. Fuqiang, HPLC-based metabolomics of Dendrobium officinale revealing its antioxidant ability, Frontiers in Plant Science (2023).
[4] L. Ming, L. Qi-Lian, H. Xiaofang, D. Xiaocui, L. Yuhan, L. Yan, F. Chongye, Hypoglycemic effects of dendrobium officinale leaves, Frontiers in Pharmacology (2023).
[5] R. Apinya, S. Ratchuporn, P. Ratchadawan, P. Thitiporn, P. Benjaporn, Evaluation of chemical compositions and biological activities of Dendrobium species, Natural Product Research (2024).
[6] P. Zhang, Z. Xingyu, Z. Xingyi, H. Yingqi, Chemical Constituents, Bioactivities, and Pharmacological Mechanisms of Dendrobium officinale: A Review of the Past Decade, Journal of Agricultural and Food Chemistry (2023).
[7] L. Changkang, S. Xincheng, S. Zhijun, S. Jun, L. Yan, W. Nan, Z. Dan, Y. Fei, D. Jungui, Chemical constituents from the stems of Dendrobium gratiosissimum and their biological activities, Phytochemistry (2022).
[8] S. Sujun, D. Peng, P. Chune, J. Haiyu, M. Longfei, P. Lizeng, Extraction, Structure and Immunoregulatory Activity of Low Molecular Weight Polysaccharide from Dendrobium officinale, Polymers (2022).
[9] H. Tao-Bin, H. Yanping, L. Yang, L. Titi, G. Wanying, W. Xuanjun, S. Jun, H. Jiang-Miao, Structural characterization and immunomodulating activity of polysaccharide from Dendrobium officinale, International Journal of Biological Macromolecules (2016).
[10] Y.J. Dong, Y.P. Zhang, X.F. Jiang, Z.Y. Xie, B. Li, N.H. Jiang, S.H. Chen, G.Y. Lv, Beneficial effects of Dendrobium officinale National Herbal Drink on metabolic immune crosstalk via regulate SCFAs-Th17/Treg, Phytomedicine 132 (2024) 155816.
[11] M. Yan, Y. Tian, M. Fu, H. Zhou, J. Yu, J. Su, Z. Chen, Z. Tao, Y. Zhu, X. Hu, J. Zheng, S. Chen, J. Chen, G. Lv, Polysaccharides, the active component of Dendrobiumofficinale flower, ameliorates chronic pharyngitis in rats via TLR4/NF-κb pathway regulation, J Ethnopharmacol 335 (2024) 118620.
[12] Y. Liyuan, L.I. De-zhi, L. Yang, Hot water extraction and artificial simulated gastrointestinal digestion of wheat germ polysaccharide, International Journal of Biological Macromolecules (2019).
[13] L. Jing, L. Wei, F. Meng-Xi, W. Anqi, W. Ding-Tao, G. Hongliang, H. Yichen, G. Ren-You, Z. Liang, L. Ying, Pressurized hot water extraction, structural properties, biological effects, and in vitro microbial fermentation characteristics of sweet tea polysaccharide, International Journal of Biological Macromolecules (2022).
[14] Z. Tang, G. Huang, H. Huang, Ultrasonic-assisted extraction, analysis and properties of purple mangosteen scarfskin polysaccharide and its acetylated derivative, Ultrasonics Sonochemistry 109 (2024).
[15] Z. Yang, L. Yihui, C. Yingying, T. Yu-Ping, X. Li, Z. Aibei, Z. Chen, Z. Shushu, Ultrasonic-assisted extraction brings high-yield polysaccharides from Kangxian flowers with cosmetic potential, Ultrasonics Sonochemistry (2023).
[16] H. Wen, L. Jie, S. Jianhua, D. Fei, Y. Aibing, Extraction of Polysaccharides from Shiitake Mushroom Based on Pineapple Enzymatic Technology, Journal of Physics: Conference Series (2024).
[17] K. Ahmed, D. Claire, Enzyme synergy for plant cell wall polysaccharide degradation, Essays in Biochemistry (2023).
[18] L. Bobo, W. Shasha, Z. Anqi, H. Qin, H. Gangliang, Ultrasound-assisted enzyme extraction and properties of Shatian pomelo peel polysaccharide, Ultrasonics Sonochemistry (2023).
[19] Y. Cholil, J. Xiaochao, C. Yu-Wen, Z. Zhuowen, G. Yuan, G. Lin, S. Danqi, R. Ilbong, W. Wenjie, W. Huimei, Ultrasound-assisted enzymatic extraction of Scutellaria baicalensis root polysaccharide and its hypoglycemic and immunomodulatory activities, International Journal of Biological Macromolecules (2023).
[20] Q. Junjie, S. Menglin, L. Siqi, Y. Qianyi, Z. Xinxin, M. Xinxin, S. Shi, W. Shaohua, Artificial neural network model- and response surface methodology-based optimization of Atractylodis Macrocephalae Rhizoma polysaccharide extraction, kinetic modelling and structural characterization, Ultrasonics Sonochemistry (2023).
[21] Z. Zhen, G. Shancai, C. Chuanding, L. Jianwei, C. Leyuan, W. Danni, H. Jun, C. Xinrui, Y. Jingyi, L. Yingying, W. Xinxuan, Optimization of extraction and bioactivity detection of celery leaf flavonoids using BP neural network combined with genetic algorithm and response, Preparative Biochemistry & Biotechnology (2021).
[22] H. DongLiang, Z. Qiang, S. KeWei, C. Gao, Z. Kun, S. Mei, W. Liang-Bi, Performance optimization of a wavy finned-tube heat exchanger with staggered curved vortex generators, International Journal of Thermal Sciences (2023).

[23] L. Haodong, X. Yan, W. Yinbo, R. Xinxiu, Z. Danyang, D. Jianying, X. Zhilong, Y. U. Shi-ying, D. Yuesheng, Dendrobium officinale Polysaccharide Prevents Diabetes via the Regulation of Gut Microbiota in Prediabetic Mice, Foods (2023).
[24] G. Xuehua, L. Shihao, W. Zhanke, Z. Guangxu, Ultrasonic-assisted extraction of polysaccharide from Dendrobium officinale: Kinetics, thermodynamics and optimization, Biochemical Engineering Journal (2022).
[25] L. Hu, Z. Xiaodan, X. Tian, L. Ranran, S. Wenjie, L. Rui, W. Tao, Z. Min, Isolation and Purification, Structural Characterization and Antioxidant Activities of a Novel Hetero-Polysaccharide from Steam Exploded Wheat Germ, Foods (2022).
[26] X. Jinrong, C. Xin, Q. Zhan, Z. Lei, H. Qiuhui, Z. Liyan, Effects of ultrasound on the degradation kinetics, physicochemical properties and prebiotic activity of Flammulina velutipes polysaccharide, Ultrasonics Sonochemistry (2022).
[27] D. Zuman, C. Chun, F. Xiong, The effect of ultrasound irradiation on the physicochemical properties and α-glucosidase inhibitory effect of blackberry fruit polysaccharide, Food Hydrocolloids (2019).
[28] L. Kecheng, X. Ronge, L. Song, Q. Yukun, Y. Huahua, L. Pengcheng, Size and pH effects of chitooligomers on antibacterial activity against Staphylococcus aureus, International Journal of Biological Macromolecules (2014).
[29] H. Ellyn, S. Martin, C. Emma, J. Emma, G. Andrew, G. Awen, T-cell modulation by cyclophosphamide for tumour therapy, Immunology (2018).
[30] O.M. Colvin, An Overview of Cyclophosphamide Development and Clinical Applications, Current Pharmaceutical Design (1999).
[31] S. Ting Ting, C. Bor-Luen, Lymphopenia, Lymphopenia-Induced Proliferation, and Autoimmunity, International Journal of Molecular Sciences, (2021).
[32] J.B. Barbara, Structure and function of red and white blood cells, Medicine (2017).
[33] Y. Sen, C. Ming, L. Qiaofei, L. Quan, Glycosylation of immunoglobin G in tumors: Function, regulation and clinical implications, Cancer Letters (2022).
[34] W.H. Timothy, R. Andrea, Production and Function of Immunoglobulin A, Annual Review of Immunology (2021).
[35] H. Toshio, IL-6 in inflammation, autoimmunity and cancer, International Immunology (2020).
[36] A.D. Charles, Overview of the IL-1 family in innate inflammation and acquired immunity, Immunological Reviews (2017).
[37] L.-S. Diogo, M.C. Guilhermina, G.C. António, R. Susana, S. Margarida, Balancing the immune response in the brain: IL-10 and its regulation, Journal of Neuroinflammation (2016).
[38] L. Kristina Berg, M.M. Malin Holm, K. Kushi, H. Charlotte Andrea Hauge, M. Asle Wilhelm, L.I. Marius, S. Birgitte, K. Dag, D.-R. Anne Margarita, T. Kjetil, R. Dag Henrik, Enhanced Gut-Homing Dynamics and Pronounced Exhaustion of Mucosal and Blood CD4+ T Cells in HIV-Infected Immunological Non-Responders, Frontiers in Immunology, (2021).
[39] K. Christina, K. May, B. Anirban, S.K. Alexander, Unique Immunoregulation of Lung Cancer by CD8+ T Cells, Journal of Immunology (2023).
[40] D.-M. Thibaut, N. Sonia, Z. Oksana, D.K. Jo Ann, B.H. Charles, M. Kara, J. E. Joseph, Acute HIV Infection and CD4/CD8 Ratio Normalization After Antiretroviral Therapy Initiation, Journal of Acquired Immune Deficiency Syndromes (2018).
[41] C. Antonio, S. Giulia, A. Francesco, M. Marcello, R. Cinzia Valeria, S. Francesco, R. Anna De, C. Chiara, V. Luigi Del, M. Vincenzo Brescia, L. Roberta, CD4/CD8 ratio during natalizumab treatment in multiple sclerosis patients, Journal of Neuroimmunology (2017).
[42] R. Raquel, M. Elena, M.S. Javier, B. Fátima, S. Talía, G. Santiago Moreno, S. V. Sergio, CD4/CD8 Ratio During Human Immunodeficiency Virus Treatment: Time for Routine Monitoring? Clinical Infectious Diseases (2023).
[43] N.K. Priscilla, How the thymus shaped immunology, Science (2020).
[44] M.L. Steven, W. Adam, C.E. Stephanie, Structure and function of the immune system in the spleen, Science Immunology (2019).
[45] W. Ching On, R.G. Steven, H. Hongxiang, C. Yufang, E.S. Victoria, H. Yuchun, L. K. David, E.G. William, J.B. Hugo, V. Kartik, Lysosomal Degradation Is Required for Sustained Phagocytosis of Bacteria by Macrophages, Cell Host & Microbe (2017).
[46] B.S. Inês, V.V. Otília, Maturation of phagosomes containing different erythrophagocytic particles in primary macrophages, FEBS Open Bio (2017).